

## Plane Stress – Finite Element Analysis and Experimental Measurement

GOGA Vladimír

Institute of Power and Applied Electrical Engineering  
Faculty of Electrical Engineering and Information Technology  
Slovak University of Technology  
Ilkovičova 3, 812 19 Bratislava  
Slovak Republic  
vladimir.goga@stuba.sk

**Keywords:** plane stress, finite element analysis, principal stress, strain gauge measurement.

**Abstract.** This paper presents new design of the structural specimen for plane stress analysis. Requirement was that the specimen is loaded by universal tensile testing machine without any special equipment. Specimen was analyzed using finite element method in ANSYS Workbench software. Finite element method was also used for simulation of strain gauge measurement to determine principal stresses, equivalent von Mises stress and orientation of the principal axes in the center of specimen. Finally, experimental stress analysis using strain gauges was performed on real specimen. Results from experimental measurements and numerical simulations were compared.

### Introduction

Plane stress is a special case of general three-dimensional stress state at a point of structure under mechanical loading. Plane stress is typical in many engineering problems where the stresses are induced in a thin plate or on the free surface of a structural element, such as the surfaces of thin-walled pressure vessels under external or internal pressure, the free surfaces of shafts in torsion, beams under transverse load, airplane fuselage and wings, car bodies etc. [1-3].

A point of thin-walled structure can be represented as a rectangular planar element in the  $x$ - $y$  plane. This element in the state of plane stress has three nonzero stress components: two normal stresses  $\sigma_x$ ,  $\sigma_y$  and one shear stress  $\tau_{xy}$  (from static equilibrium  $\tau_{xy} = \tau_{yx}$ ) as shown in Fig. 1. In three-dimensional state of stress, there are other three stress components  $\sigma_z$ ,  $\tau_{yz}$ ,  $\tau_{zx}$  in perpendicular direction to the  $x$ - $y$  plane ( $z$  direction), but these ones are zero in the case of plane stress.

Stress components  $\sigma_x$ ,  $\sigma_y$  and  $\tau_{xy}$  vary with the angle  $\varphi$  of rotation of the element into new coordinate system. In new coordinate system, there are maximum  $\sigma_1$  and minimum  $\sigma_2$  normal stresses called principal stresses and zero shear stress in the element, see Fig. 1. Principal stresses lie in principal directions. Maximum shear stress  $\tau_{max}$  occurs when the element is rotated from principal directions about angle  $45^\circ$ , see Fig. 1. For this orientation of element, there are except maximum shear stress  $\tau_{max}$  also two nonzero normal stresses with the same average stress value  $\sigma_{ave}$ .

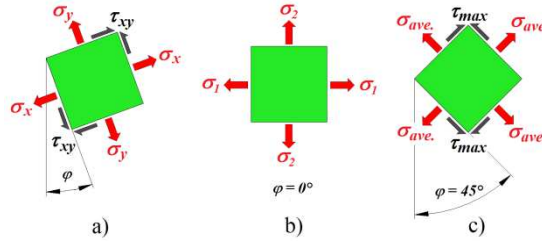


Fig. 1. Element in the state of plane stress:

a) x-y coordinate system, b) principal directions, c) direction of maximum shear stress.

In general, there are different values of normal and shear stresses in any coordinate system of the element. This transformation of stress in order to angle  $\varphi$  describes Mohr's circle. In Mohr's circle the horizontal axis represents normal stress and vertical axis represents shear stress in the element. Normal and shear stresses in current coordinate system of the element are represented by a point on a circle. Angle  $\varphi$  is twice in the center of circle, see Fig. 2.

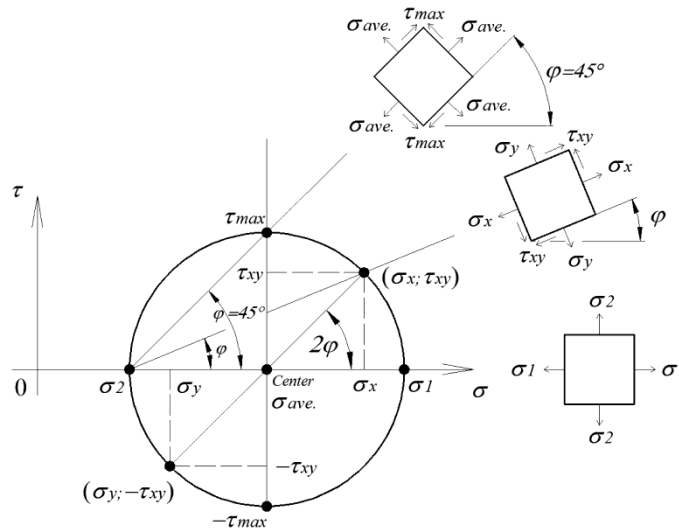


Fig. 2. Mohr's circle for plane stress.

If all three stress components for any coordinate system are known, then the principal stresses  $\sigma_{1,2}$ , maximum shear stress  $\tau_{max}$ , average stress  $\sigma_{ave}$  and angle  $\varphi$  with respect to principal directions are defined as follows [1-3]:

$$\begin{aligned} \sigma_{1,2} &= \frac{(\sigma_x + \sigma_y)}{2} \pm \sqrt{\left(\frac{\sigma_x - \sigma_y}{2}\right)^2 + \tau_{xy}^2} & \tan(2\varphi) &= \frac{2\tau_{xy}}{\sigma_x - \sigma_y} \\ \tau_{max} &= \pm \sqrt{\left(\frac{\sigma_x - \sigma_y}{2}\right)^2 + \tau_{xy}^2} = \pm \frac{(\sigma_1 - \sigma_2)}{2} & \sigma_{ave} &= \frac{(\sigma_x + \sigma_y)}{2} \end{aligned} \quad (1)$$

If principal stresses are known or calculated from Eq. 1, the von Mises criterion  $\sigma_{Mises}$  (ductile materials) or maximum normal stress criterion  $\sigma_{max}$  (brittle materials) can be used to compare plane stress with uniaxial yield stress  $\sigma_Y$  and ultimate tensile strength  $\sigma_{TS}$  [1,2]:

$$\sigma_{Mises} = \sqrt{\sigma_1^2 - \sigma_1\sigma_2 + \sigma_2^2} \leq \sigma_Y \quad \sigma_{max} = \sigma_1 \leq \sigma_{TS} \quad (2)$$

Experimental determination of mechanical stresses is performed by measuring of the strains. In the state of plane stress there are stress components only in x-y plane but strains are

in all three directions. Normal stresses produce normal strains  $\varepsilon_x$ ,  $\varepsilon_y$ ,  $\varepsilon_z$  ( $\varepsilon_z$  is result of Poisson's ratio effect) and shear stress produces shear strain  $\gamma_{xy}$  in  $x$ - $y$  plane. In the region of elastic deformation we assume the linear strain-stress relationship defined by generalized Hooke's law. Hooke's law for plane stress is given by the equation ( $\varepsilon_z$  is not considered) [1-3]:

$$\begin{bmatrix} \varepsilon_x \\ \varepsilon_y \\ \gamma_{xy} \end{bmatrix} = \frac{1}{E} \begin{bmatrix} 1 & -\nu & 0 \\ -\nu & 1 & 0 \\ 0 & 0 & 2(1+\nu) \end{bmatrix} \begin{bmatrix} \sigma_x \\ \sigma_y \\ \tau_{xy} \end{bmatrix} \Leftrightarrow \begin{bmatrix} \sigma_x \\ \sigma_y \\ \tau_{xy} \end{bmatrix} = \frac{E}{1-\nu^2} \begin{bmatrix} 1 & \nu & 0 \\ \nu & 1 & 0 \\ 0 & 0 & \frac{1-\nu}{2} \end{bmatrix} \begin{bmatrix} \varepsilon_x \\ \varepsilon_y \\ \gamma_{xy} \end{bmatrix} \quad (3)$$

where  $E$  is Young's modulus and  $\nu$  is Poisson's ratio.

The strains on a surface of body are usually most conveniently measured by means of electric-resistance strain gauges. The simplest form of such a gauge is a short length of wire insulated from and glued to the surface. When stretching occurs the resistance of the wire is increased, and the strain can thus be measured electrically. Single strain gauge is capable only of measuring the extensional strain in the direction that the gauge is oriented. Therefore, if the principal directions are known the gauges are mounted in these directions (principal strains  $\varepsilon_1$  and  $\varepsilon_2$  are measured) and principal stresses can be calculated as follows [1]:

$$\sigma_1 = \frac{E}{(1-\nu^2)}(\varepsilon_1 + \nu\varepsilon_2) \quad \sigma_2 = \frac{E}{(1-\nu^2)}(\varepsilon_2 + \nu\varepsilon_1) \quad (4)$$

When the principal directions are not known in advance, three measurements are needed. In this case, to determine the state of plane stress it is necessary measure not only two extensional strains, but also the shear strain, with respect to some given  $x$ - $y$  coordinate system. However, there is not direct way to measure the shear strain. [1]

The solution of this problem is to make three independent measurements of extensional strains at a point on the surface of structure. The most obvious approach is to place three strain gauges together in a rosette with each gauge oriented in a different direction and with all of them located as close together as possible to approximate a measurement at a point [1]. Strain gauges in rosette are typically oriented at fixed angle  $45^\circ$  (rectangular rosette) or  $60^\circ$  (delta rosette) with respect to each other.

Fig. 3 shows measurement with rectangular strain gauge rosette. Gauge A is rotated relative to the principal axis 1 of the angle  $\varphi$ . Directions of gauges A and C represents  $x$ - $y$  coordinate system of the element.

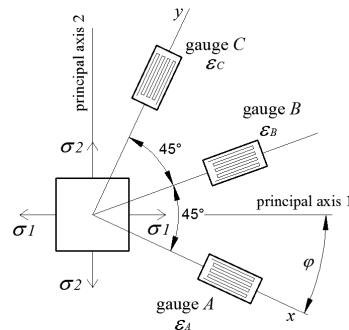


Fig. 3. Measurement with rectangular strain gauge rosette.

From measured strains  $\varepsilon_A$ ,  $\varepsilon_B$ ,  $\varepsilon_C$  we can determine strain components for element in  $x$ - $y$  coordinate system [1]:

$$\varepsilon_x = \varepsilon_A \quad ; \quad \varepsilon_y = \varepsilon_C \quad ; \quad \gamma_{xy} = 2\varepsilon_B - \varepsilon_A - \varepsilon_C \quad (5)$$

Now, it is possible calculate stresses in the element in  $x$ - $y$  coordinate system using generalized Hooke's law, Eq. 3. Principal stresses  $\sigma_{1,2}$ , maximum shear stress  $\tau_{max}$  and angle  $\varphi$  between principal directions and  $x$ - $y$  coordinate system are then calculated from Eq. 1. The von Mises stress is calculated from Eq.2.

### Plane stress testing methods

Plane stress is tested using various methods. The most common test is biaxial tensile test of thin cruciform specimen as shown in Fig. 4a. Arms of cruciform specimen are loaded in tension. There are principal axes in the directions of applied loads in the center of specimen. Testing machines for this test require combination of two or four individual force actuators as shown in Fig. 4b. It is also possible use universal tensile testing machine with special pantograph device, see Fig. 4c.

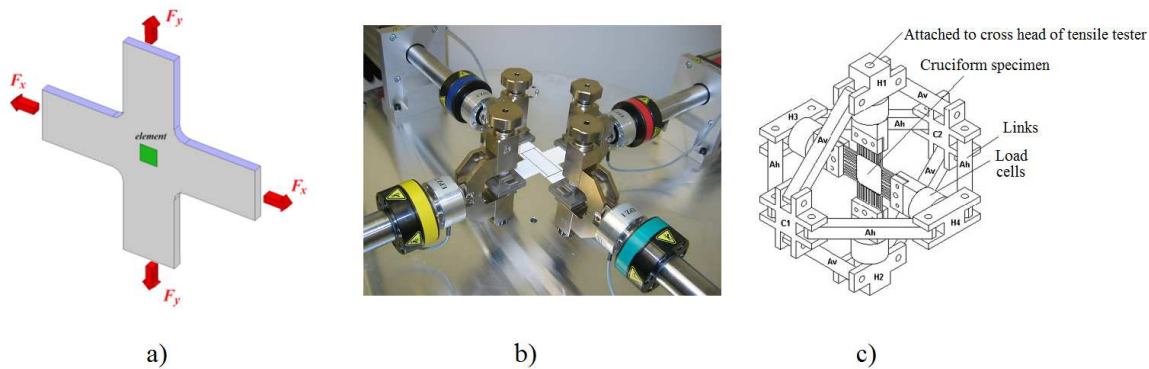


Fig. 4. Biaxial tensile test: a) cruciform specimen, b) tension in two directions by action of four actuators [4,5], c) pantograph mechanism for tensile testing machine [6,7].

Arcan et al. [8] proposed a biaxial fixture, commonly known as the Arcan fixture, to produce biaxial states of stress. Specimen with butterfly geometry is usually used, see Fig. 5a. The Arcan fixture can be used to apply both shear and axial forces to the test specimen, see Fig. 5b [9].

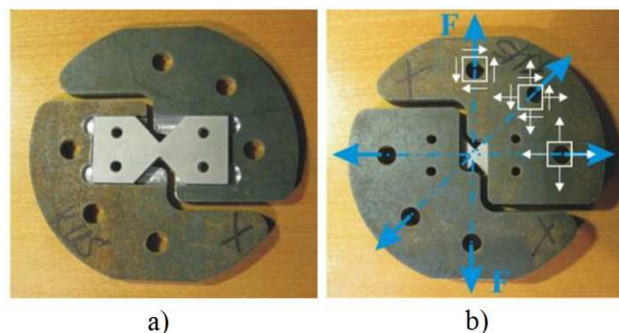


Fig. 5. Arcan fixture [10]: a) butterfly specimen, b) biaxial states of stress.

Different type of specimen is thin tubular specimen loaded by axial tension force and inertial pressure as shown Fig. 6a. Plane stress state is enforced in the shell of the tubular specimen. Device for testing this kind of specimen requires additional hydraulic pump or pneumatic compressor, Fig. 6b.

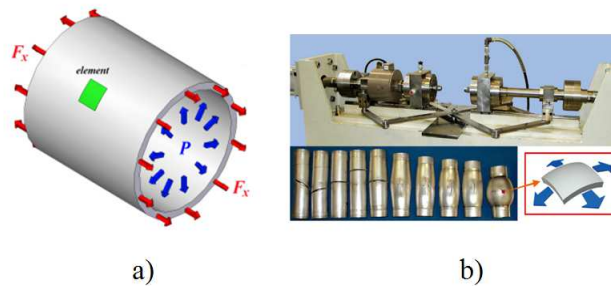


Fig. 6. Testing of tubular specimen: a) tubular specimen, b) servo-controlled tube-bulging testing machine [11].

All these testing methods are quite complicated or expensive so our target was design new specimen for plane stress analysis which will be testing by using just universal tensile test machine. Software ANSYS Workbench was used for design the specimen shape. Experimental measurement using strain gages was consecutively performed.

### New specimen for plane stress investigation

In Fig. 7, there is a design of new specimen for testing plane stress state. This specimen can be tested using universal tensile testing machine without any special equipment. Vertical arm is loaded in tension and we assumed that due to specimen design the horizontal arm is loaded in compression. In the center of specimen the principal directions should be in the vertical and horizontal directions as shown in Fig. 7. This assumption was verified by finite element analysis.

Parameters for plane stress test:

- shape and dimensions (in millimeters) of the specimen are shown in Fig. 7;
- thickness of the specimen:  $t = 1$  mm;
- material: aluminum ( $E = 70$  GPa,  $\nu = 0.33$ );
- applied force:  $F = 200, 400, 600$  N.

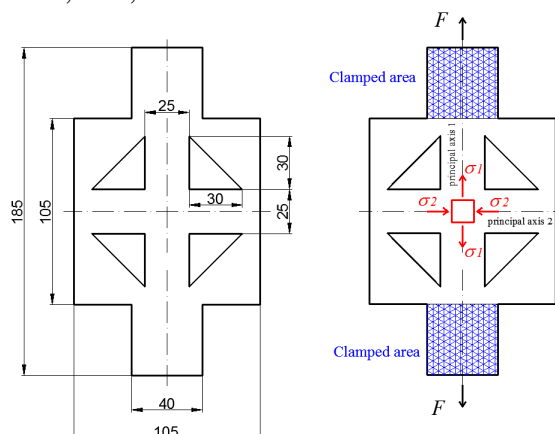


Fig. 7. Shape of the specimen.

Static structural finite element analysis (FEA) was performed in software ANSYS Workbench [12]. The specimen was modeled as surface body. Type of structural analysis was plane stress with thickness. The main target of this analysis was determined whether the principal axes in the center of specimen are in vertical and horizontal directions. This assumption was confirmed from the vector plot of deformation and principal directions in the center of specimen, see Fig. 8.

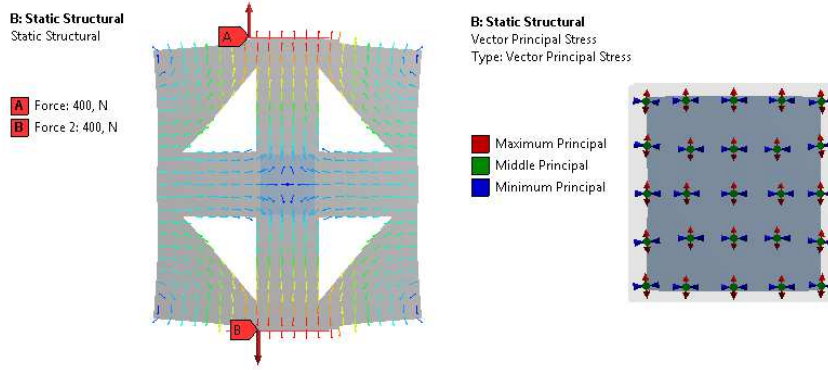


Fig. 8. Vector plot of deformation and principal directions in the center of specimen.

Results of deformation and state of stress for the entire specimen and for a point in the specimen center are in Fig. 9 (load case  $F = 400$  N). Results for all load cases are in Tab. 1.

Tab. 1. Results from static structural FEA.

$F$	$\sigma_1$	$\sigma_2$	$\tau_{max}$	$\sigma_{Mises}$
[N]	[MPa]	[MPa]	[MPa]	[MPa]
200	5.0	-2.0	4.0	7.1
400	11.7	-4.2	7.9	14.2
600	17.5	-6.3	11.9	21.3

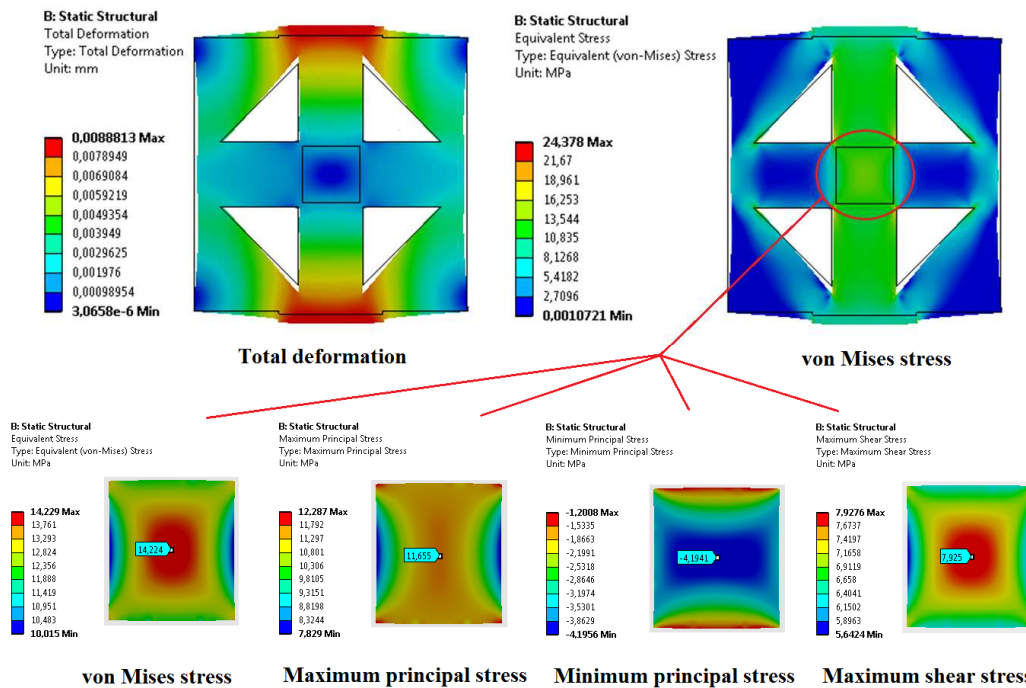


Fig. 9. Plot results for load case  $F = 400$  N.

### Finite element simulation of strain gauge measurement

Rectangular strain gauge rosette was modeled in the center of specimen to determine three individual extensional strains. Orientation of the rosette is shown in Fig. 10. Gauge A is rotated from principal axis 2 about angle  $\varphi = -20^\circ$ . Specimen was modeled as three-dimensional body and each gauge was modeled as individual plane element with own local coordinate system. Results of this simulation were extensional strains of individual gauges  $\varepsilon_A$ ,  $\varepsilon_B$ ,  $\varepsilon_C$  (X axis of local coordinate system, see Fig. 10). Stress quantities were calculated from the strain results using Eq. 1-3 and 5. All results are presented in Tab. 2.

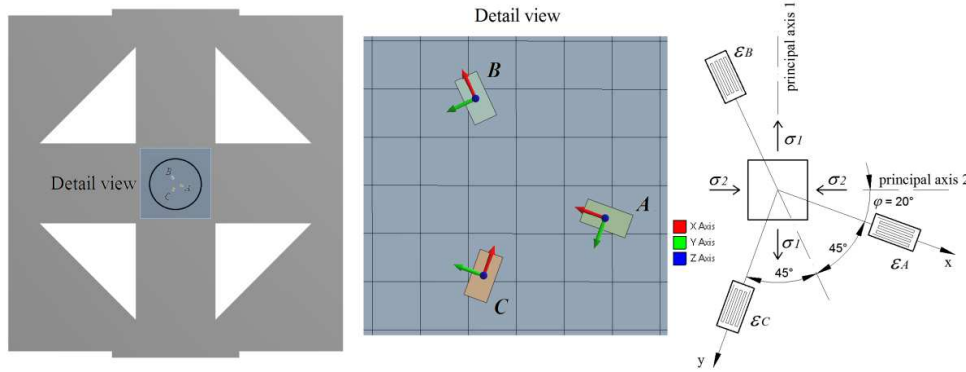


Fig. 10. Orientation of the strain gauges.

Tab. 2. Results from simulation of strain gauge measurement.

$F$	$\epsilon_A$	$\epsilon_B$	$\epsilon_C$	$\sigma_x$	$\sigma_y$	$\tau_{xy}$	$\sigma_1$	$\sigma_2$	$\tau_{max}$	$\sigma_{Mises}$	$\varphi$
[N]	[ $\mu\text{m}/\text{m}$ ]	[ $\mu\text{m}/\text{m}$ ]	[ $\mu\text{m}/\text{m}$ ]	[MPa]	[MPa]	[MPa]	[MPa]	[MPa]	[MPa]	[MPa]	[ $^\circ$ ]
200	-39.6	65.7	74.9	-1.2	4.9	2.5	5.8	-2.1	3.9	7.1	-20
400	-79.1	131.4	149.8	-2.3	9.7	5.1	11.6	-4.2	7.9	14.1	-20
600	-118.7	197.1	224.7	-3.5	14.6	7.6	17.3	-6.3	11.8	21.2	-20

### Experimental strain gauge measurement

Real specimen was subjected to testing. Three gauges were attached on the specimen. Orientation of gauges is the same as in previous finite element simulation, see Fig. 11. Measured strains and calculated stresses are in Tab. 3.

Devices used for experimental measurements: universal tensile testing machine, load cell, strain gauges, measuring amplifier, PC with software to acquisition and visualization of measuring data.

Tab. 3. Results from experimental measurement.

$F$	$\epsilon_A$	$\epsilon_B$	$\epsilon_C$	$\sigma_x$	$\sigma_y$	$\tau_{xy}$	$\sigma_1$	$\sigma_2$	$\tau_{max}$	$\sigma_{Mises}$	$\varphi$
[N]	[ $\mu\text{m}/\text{m}$ ]	[ $\mu\text{m}/\text{m}$ ]	[ $\mu\text{m}/\text{m}$ ]	[MPa]	[MPa]	[MPa]	[MPa]	[MPa]	[MPa]	[MPa]	[ $^\circ$ ]
200	-40.4	61.6	68.6	-1.4	4.3	2.5	5.3	-2.3	3.8	6.8	-20.5
400	-80.8	123.2	137.2	-2.8	8.7	5.0	10.6	-4.7	7.6	13.5	-20.5
600	-121.2	184.8	205.8	-4.2	13.0	7.5	15.8	-7.0	11.4	20.3	-20.5

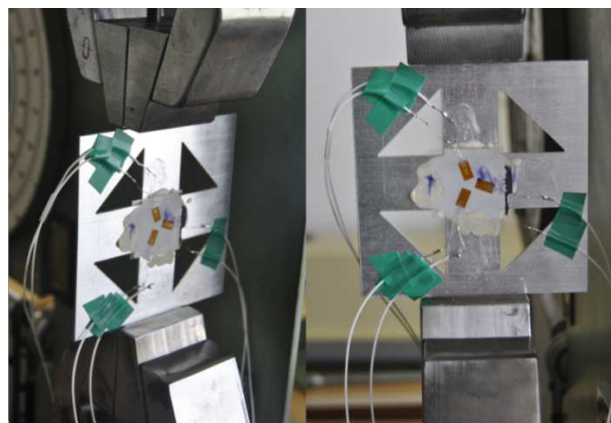


Fig. 11. Real specimen with strain gauges.

### Conclusion

New specimen for plane stress testing was designed. Finite element method was used for analysis the state of stress in the center of specimen. Finite element simulation of strain gauge measurement was also performed. Finally experimental measurement was done. Results from simulations are compared with experimental results in Tab. 4 and Tab. 5. Percentage errors of

both finite element analyses are less than 15 % in view of the measurements. Von Mises stress errors are even smaller than 6 %. Results differences are acceptable and we can consider that shape of the specimen is suitable for analysis of plane stress state. Advantage of this specimen is that specimen can be tested by using universal tensile testing machine without any special equipment. Different stress values can be achieved by changing of the specimen dimensions.

Tab. 4. Comparison of static structural FEA and measurements.

$F$	[N]	200			400			600		
		FEA	Measured	$\Delta$ [%]	FEA	Measured	$\Delta$ [%]	FEA	Measured	$\Delta$ [%]
$\sigma_1$	[MPa]	5.0	5.3	<b>5.7</b>	11.7	10.6	<b>-10.4</b>	17.5	15.8	<b>-10.8</b>
$\sigma_2$	[MPa]	-2.0	-2.3	<b>13.0</b>	-4.2	-4.7	<b>10.6</b>	-6.3	-7.0	<b>10.0</b>
$\tau_{max}$	[MPa]	4.0	3.8	<b>-5.3</b>	7.9	7.6	<b>-3.9</b>	11.9	11.4	<b>-4.4</b>
$\sigma_{Mises}$	[MPa]	7.1	6.8	<b>4.4</b>	14.2	13.5	<b>-5.2</b>	21.3	20.3	<b>-4.9</b>

Tab. 5. Comparison of strain gauge simulations ( $G_{FEA}$ ) and measurements.

$F$	[N]	200			400			600		
		$G_{FEA}$	Measured	$\Delta$ [%]	$G_{FEA}$	Measured	$\Delta$ [%]	$G_{FEA}$	Measured	$\Delta$ [%]
$\sigma_1$	[MPa]	5.8	5.3	<b>-9.4</b>	11.6	10.6	<b>-9.4</b>	17.3	15.8	<b>-9.5</b>
$\sigma_2$	[MPa]	-2.1	-2.3	<b>8.7</b>	-4.2	-4.7	<b>10.6</b>	-6.3	-7.0	<b>10.0</b>
$\tau_{max}$	[MPa]	3.9	3.8	<b>-2.6</b>	7.9	7.6	<b>-3.9</b>	11.8	11.4	<b>-3.5</b>
$\sigma_{Mises}$	[MPa]	7.1	6.8	<b>4.4</b>	14.1	13.5	<b>-4.4</b>	21.2	20.3	<b>-4.4</b>
$\varphi$	[°]	-20	-20.5	<b>2.4</b>	-20	-20.5	<b>2.4</b>	-20	-20.5	<b>2.4</b>

## Acknowledgement

This work was supported by Grant Agency KEGA, grant No. 015STU-4/2012 and grant VEGA 1/0534/12.

## References

- [1] O.A. Bauchau, J.I. Craig, Structural Analysis: With Applications to Aerospace Structures, Publisher: Springer, ISBN 978-90-481-2515-9, 2009
- [2] A.C. Ugural, S.K. Fenster, Advanced Mechanics of Materials and Applied Elasticity, Publisher: Prentice Hall, ISBN 978-0-13-707920-9, 2011
- [3] S. Timoshenko, J.N. Goodier, Theory of Elasticity, McGraw-Hill Book Company, 1951
- [4] Information on <http://ase.tufts.edu/msml/resourcesBiaxial.asp>
- [5] Information on <http://www.qualitymag.com/articles/86201-case-studies-testing-a-soft-body-robot>
- [6] A. Hannon, P. Tiernan, A review of planar biaxial tensile test systems for sheet metal, Journal of Material Processing Technology, vol. 198, Issues 1-3, 2008
- [7] G. Ferron, A. Makinde, Design and development of a biaxial strength testing device, Journal of Testing and Evaluation, vol. 16, Issue 3, 1988
- [8] M. Arcan, Z. Hashin, A. Voloshin, A method to produce uniform plane-stress state with applications to fiber-reinforced materials, Experimental Mechanics, vol. 18, Issue 4, 1978, pp. 141-146
- [9] R. El-Hajjar, R. Haj-Ali, In-plane shear testing of thick-section pultruded FRP composites using a modified Arcan fixture, Composites Part B: Engineering, vol. 35, Issue 5, 2004, pp. 421-428,
- [10] M. Kalina, F. Šimčák, Stress and strain field analysis by method ESPI with use of fixture for shear test Arcan, Applied mechanics, 15<sup>th</sup> international conference, (2013)
- [11] Information on [http://www.tuat.ac.jp/~mech/english/research\\_digital.html](http://www.tuat.ac.jp/~mech/english/research_digital.html)
- [12] ANSYS, Theory manual for Workbench, 2011